Journal of Alloys and Compounds 480 (2009) 35–39

Contents lists available at ScienceDirect

Journal of Alloys and Compounds

journal homepage: www.elsevier.com/locate/jallcom

# Direct observation of remarkable crystalline-electric-field effect in quasi-two-dimensional antiferromagnet $Er_5Ir_4Si_{10}$ single crystal by low-temperature specific heat

K. Tsutsumi [a,*], S. Nimori [b], G. Kido [b]

[a] Department of Physics, Kanazawa University, Kanazawa 920-1192, Japan
[b] Tsukuba Magnet Laboratory, National Institute of Materials Science, 3-13 Sakura, Tsukuba, Ibaragi 305-0003, Japan

ARTICLE INFO

*Article history:*
Received 22 July 2008
Received in revised form
11 September 2008
Accepted 17 September 2008
Available online 20 November 2008

*PACS:*
75.50.−y
75.50.Ee
75.30.Gw

*Keywords:*
Quasi-two-dimensional antiferromagnet
Crystalline-electric-field effect

ABSTRACT

We have intensively investigated the antiferromagnetic phase transition in the ternary rare-earth metal silicide $Er_5Ir_4Si_{10}$ single crystal by performing the high-resolution measurement of the low-temperature specific heat under zero-magnetic field and the AC magnetization. In the temperature dependence of important physical quantities associated with the antiferromagnetic phase transition, we have observed anomalies with the antiferromagnetic long-range ordering at Neel temperature $T_N$. We have confirmed that $T_N$ is 3.5 K. In addition, we have first observed two surprising results. Firstly, a shoulder was observed in the vicinity of 2 K in addition to the sharp peak at $T_N$ corresponding to the antiferromagnetic phase transition in the high-resolution measurement of the low-temperature specific heat. Secondly, the anomaly of the AC magnetization at $T_N$ depends to the magnetic field direction. We have clearly observed the anomaly of the AC magnetization at $T_N$ when the AC magnetic field orientation is parallel to the *c*-axis, whereas we have observed no anomaly of the AC magnetization at $T_N$ when the AC magnetic field orientation is perpendicular to the *c*-axis. These results clarify that our $Er_5Ir_4Si_{10}$ single crystal is a quasi-two-dimensional antiferromagnet and has no three-dimensional magnetic structure of the $Er^{3+}$ local moments. However, we have observed a peak of the AC magnetization around 2 K when the AC magnetic field orientation is perpendicular to the *c*-axis. This temperature corresponds to that at which a shoulder is observed in the measurement of the low-temperature specific heat. Furthermore, we have observed no frequency dependence of the AC magnetization which is ordinarily observed in the spin glass state. This result means that there is no disorder in our $Er_5Ir_4Si_{10}$ single crystal because the crystal structure of $Er_5Ir_4Si_{10}$ has the tetragonal crystal structure in which the octagons of $Er^{3+}$ ions are stacked. In addition, both tetragons and octagons of $Er^{3+}$ local moments have no magnetic frustration. At last we can conclude that both the shoulder of the low-temperature specific heat in the vicinity of 2 K and the peak of the AC magnetization around 2 K, which is only observed when the AC magnetic field orientation is perpendicular to the *c*-axis, correspond to the crystalline-electric-effect in the plane which is perpendicular to the *c*-axis of the tetragonal crystal structure.



## 1. Introduction

Recently, the ternary rare-earth metal silicide $R_5Ir_4Si_{10}$ ($R$ = heavy rare-earth metal, Sc and Lu) has been intensively studied. The attractive phenomena in this ternary compound are antiferromagnetic phase transition [1–7], superconducting phase transition [1,8–15], charge-density wave phase transition [16–29] and the nuclear magnetism [7]. This compound group crystallizes in the tetragonal $Sc_5Co_4Si_{10}$-type crystal structure and the space group is *P*4/*mbm* [1,7,15]. The projection of $Er_5Ir_4Si_{10}$ crystal structure along the *c*-axis is shown in Fig. 1. The features of this crystal structure are the absence of the cluster which is composed of the transition metals and the direct bond between the transition metals. These features are in contrast to those of Cheverel phase chalcogenides $RMo_6S_8$ ($R$ = rare-earth metal) and rhodium boride compounds $RRh_4B_4$ ($R$ = rare-earth metal). In the $R_5Ir_4Si_{10}$ compound group, the Ir atoms and the Si atoms form planar nets of pentagons and hexagons that are linked in the plain which is perpendicular to the *c*-axis and then connected along the *c*-axis via Ir–Si–Ir zigzag chains. On the other hand, the rare-earth metal $R^{3+}$ ions have three sites whose symmetries are different each other. The rare-earth metal $R^{3+}$ ions at two sites of them make the octag-

* Corresponding author. Tel.: +81 76 264 5666; fax: +81 76 264 4879.
*E-mail address:* kitomi@kenroku.kanazawa-u.ac.jp (K. Tsutsumi).

0925-8388/$ – see front matter © 2008 Elsevier B.V. All rights reserved.
doi:10.1016/j.jallcom.2008.09.185

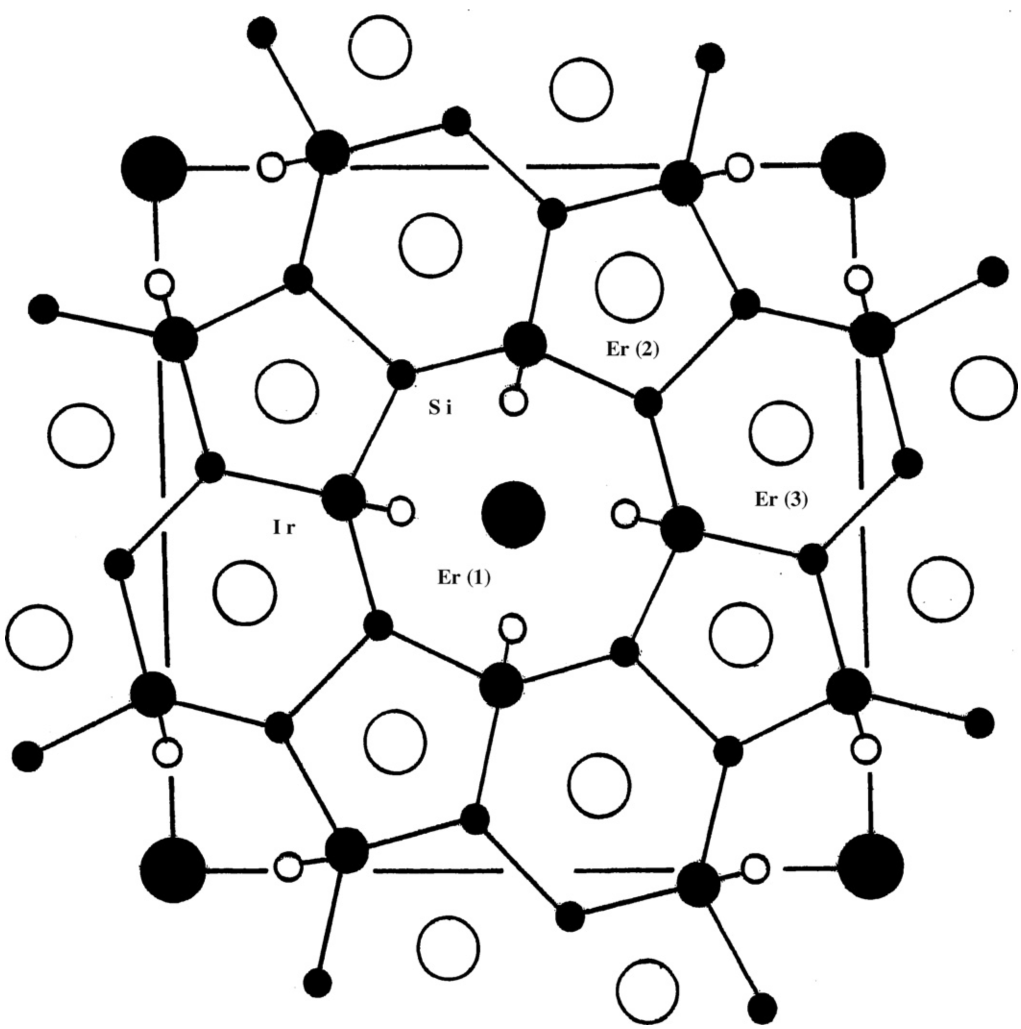


**Fig. 1.** Projection of $Er_5Ir_4Si_{10}$ along the *c*-axis whose crystal structure is $Sc_5Co_4Si_{10}$-type tetragonal one. Filled circles correspond to $z = 0$, 1 and open circles to $z = 1/2$ where *z* is the fractional coordinate along the *c*-axis of the tetragonal crystal structure.

onal layers which are perpendicular to the *c*-axis. We must note that the octagonal layer of the rare-earth metal $R^{3+}$ ions has no magnetic frustration. The rare-earth metal $R^{3+}$ ions at the third site which are present at the center of the octagons which are composed of Ir atoms and Si atoms also make another layer which is also perpendicular to the *c*-axis and a square lattice. We must also note that the square lattice of the $R^{3+}$ ions has no magnetic frustration. These two layers are perpendicular to the *c*-axis, whereas the difference between them is as follows.

The one layer contains only the rare-earth metal $R^{3+}$ ions and separates the pentagon, hexagon and octagon net works which are composed of Ir atoms and Si atoms. Another layer includes not only the rare-earth metal $R^{3+}$ ions but also the Ir atoms and Si atoms.

These results mean that there are two kinds of layers which contain the rare-earth metal $R^{3+}$ ions and perpendicular to the *c*-axis. Therefore, we must consider that the character of the $R_5Ir_4Si_{10}$ compounds is quasi-two-dimensional rather than one-dimensional on the heavy rare-earth metal $R^{3+}$ ions that correspond to the magnetic properties. Furthermore, all Ir–Si and Si–Si distances are clearly short and indicative of the covalent bonding. In many other ternary rare-earth metal silicides such as $ThCr_2Si_2$, $CeNiSi_2$ and $LaRe_2Si_2$, the net work of the Si atoms and the transition metals exists. In this article, we report and discuss the anomalies in the low-temperature specific heat and the AC magnetization measurements associated with antiferromagnetic long-range ordering in our high-quality $Er_5Ir_4Si_{10}$ single crystal.

## 2. Experimental

The $Er_5Ir_4Si_{10}$ single crystals employed in our study were grown by Czochoralski pulling method with a tetra-arc furnace in the high-purity argon atmosphere whose purity is 6N. The purity of starting materials is as follows. The purity of Si is 6N and that of Ir is 4N. However, the purity of Er is 3N. During the single crystal growth the clear facets have been observed sometimes. We confirmed as-grown crystals to be single crystals by the transmission Laue X-ray photograph method. The single crystals orient along the *c*-axis. In addition, in order to improve the quality of the as-grown single crystals we used a solid state electro-transport method (SSE). In the SSE process of the as-grown single crystal, we have kept then at 1273 K for a month.

For the measurement of the temperature dependence of the AC magnetization, we have used the commercial Quantum Design SQUID magnetometer (MPMS) from 1.8 to 20 K.

For the measurement of the temperature dependence of the low-temperature specific heat, a handmade adiabatic method has been employed. This non-commercial apparatus enables us the high-resolution measurement of the low-temperature specific heat down to 0.5 K.

## 3. Results and discussion

In Figs. 2 and 3, we show the temperature dependence of the AC magnetization from 1.8 to 20 K. We show the result in Fig. 2 when the AC magnetic field direction is parallel to the *c*-axis and

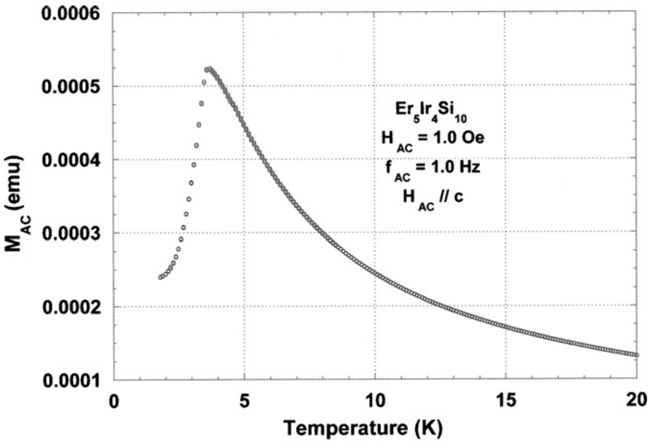


**Fig. 2.** Temperature dependence of the AC magnetization in $Er_5Ir_4Si_{10}$ single crystal when the AC magnetic field direction is parallel to the *c*-axis. We must note that there is no anomaly of the AC magnetization around 2 K.

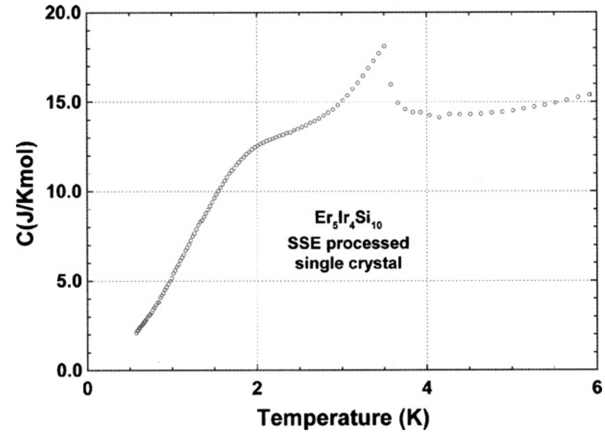


**Fig. 4.** Temperature dependence of the low-temperature specific heat in our SSE processed $Er_5Ir_4Si_{10}$ single crystal.

we show the result in Fig. 3 when magnetic field orientation is perpendicular to the *c*-axis. When the AC field orientation is parallel to the *c*-axis, $T_N$ is 3.5 K which is precisely consistent with the result of the low-temperature specific heat measurement as it is clearly shown in Fig. 4. However, we have no anomaly of the AC magnetization at $T_N$ when the AC magnetic field direction perpendicular to the *c*-axis as it is very clearly shown in Fig. 4. When we take the results mentioned just above into consideration, we must conclude that our $Er_5Ir_4Si_{10}$ single crystals have no three-dimensional magnetic structure of $Er^{3+}$ local moments. This statement is completely different from those which are described in Ref. [18].

In addition, we have observed the peak of the AC magnetization around 2 K when the AC magnetic field orientation is perpendicular to the *c*-axis. We have already reported that *a shoulder* is observed in the temperature dependence of the low-temperature specific heat in the vicinity of 2 K [7]. *A shoulder* in the vicinity of 2 K is very precisely consistent with the peak around 2 K in the temperature dependence of the AC magnetization when the AC magnetic field direction is perpendicular to the *c*-axis. At last we have completely confirmed that *a shoulder* corresponds to the magnetic property in the plane which is perpendicular to the *c*-axis of $Er_5Ir_4Si_{10}$ single crystal. This result reveals that $Er_5Ir_4Si_{10}$ single crystal is a quasi-two-dimensional material and a quasi-two-dimensional antiferromagnet.

Next, we must discuss on the relation between *a shoulder* in the temperature dependence of the low-temperature specific heat in the vicinity of 2 K and the peak of the AC magnetization around 2 K when the AC magnetic field orientation is perpendicular to the *c*-axis. *A shoulder* suggests that the magnetic spatial ordering is a short-range one. The representative magnetic short-range ordering is the spin glass state. The AC magnetization measurement is very powerful for the investigation of the spin glass behavior. We have performed the frequency dependence measurement of the AC magnetization by using the AC magnetic field whose orientation is perpendicular to the *c*-axis. The results are shown in Fig. 5. We have observed no spin glass like behavior. Namely, the peak of the AC magnetization does not shift to higher temperature and the AC magnetization rapidly decreases with increasing the frequency of the AC magnetic field. These results means that there is no spin glass state in our $Er_5Ir_4Si_{10}$ single crystal. Non-existence of the spin glass state verifies that there is no disorder in our $Er_5Ir_4Si_{10}$ single crystal because the crystal structure of $R_5Ir_4Si_{10}$ ($R$ = Tb, Dy, Ho, Er) has no magnetic frustration. Therefore, we can conclude that *a shoulder* in the vicinity of 2 K in the temperature dependence of the low-temperature specific heat and the peak of the AC magnetization when the AC magnetic field orientation is perpendicular

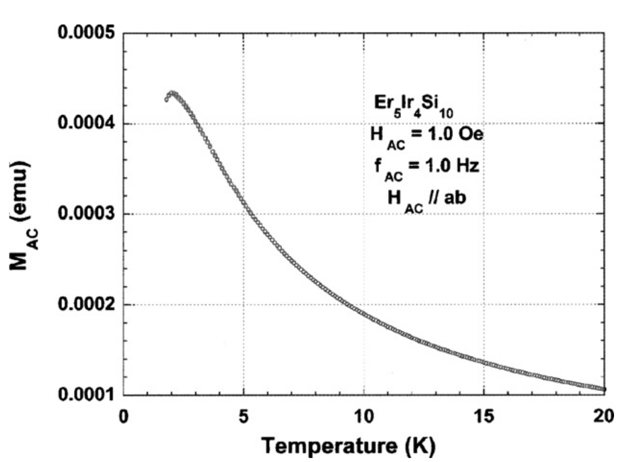


**Fig. 3.** Temperature dependence of the AC magnetization in $Er_5Ir_4Si_{10}$ single crystal when the AC magnetic field direction is perpendicular to the *c*-axis. We must note that there is no anomaly of the AC magnetization at $T_N$ = 3.5 K.

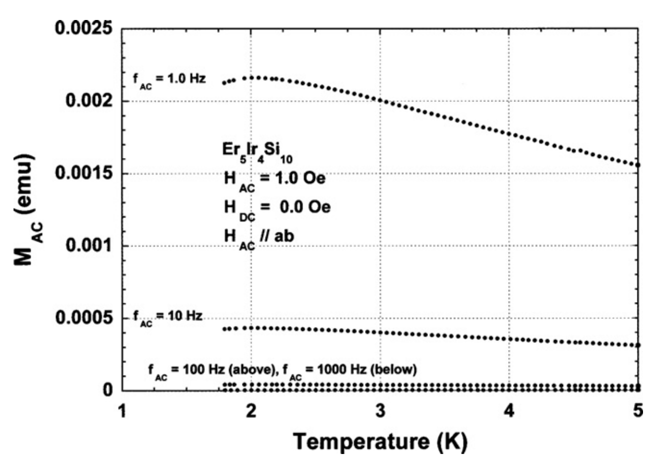


**Fig. 5.** Frequency dependency of the AC magnetization when the magnetic field direction is perpendicular to the *c*-axis. The measurements have been performed at 1.0, 10, 100 and 1000 Hz, respectively. No spin glass behavior has observed. We must note that no spin glass behavior clarifies that there is no disorder in our SSE processed $Er_5Ir_4Si_{10}$ single crystal.

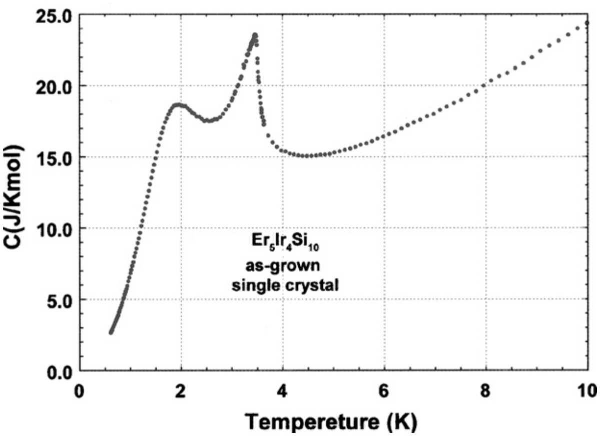


**Fig. 6.** Temperature dependence of the low-temperature specific heat in the as-grown $Er_5Ir_4Si_{10}$ single crystal grown by Czochoralski pulling method. We must note that two successive peaks are observed.

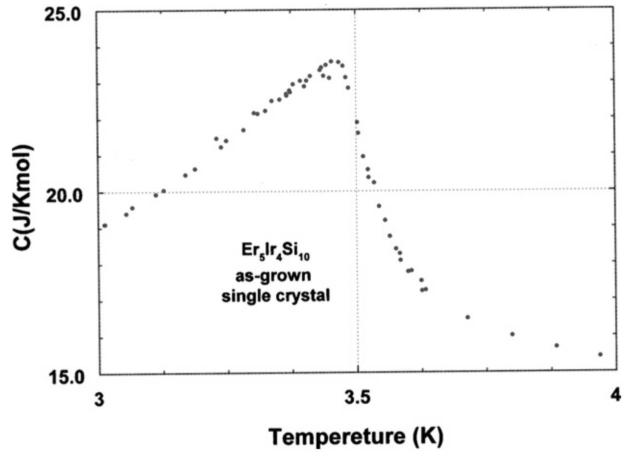


**Fig. 7.** The temperature-higher peak in the temperature dependence of the low-temperature specific heat of the as-grown $Er_5Ir_4Si_{10}$ single crystal grown by Czochoralski pulling method. We must note that the temperature-higher peak is observed at a little lower temperature than 3.5 K which is $T_N$ in our SSE processed single crystal as is clearly shown in Fig. 4.

to the *c*-axis originate from the crystalline-electric-field effect in the plane of $Er_5Ir_4Si_{10}$ single crystal which is perpendicular to the *c*-axis.

Galli et al. [16–18] had reported that the high-quality single crystal of $Er_5Ir_4Si_{10}$ single crystal undergoes the long-range antiferromagnetic transition at 2.8 K from the DC magnetization measurement by using Quantum Design MPMS, the measurements of the resistivity and the specific heat by Quantum Design PPMS and the neutron diffraction study. These measurements by using Quantum Design MPMS and PPMS only down to 1.8 K cannot clearly detect *a shoulder* in the low-temperature specific heat [7] and the AC magnetization peak around 2 K which we have first observed and reported in this article. We strongly insist that the original finding mentioned just above originates from the high quality of our SSE processed single crystals. In fact, $T_N$ is 3.5 K of our samples, whereas $T_N$ of the high-quality single crystal prepared by Galli et al. is 2.8 K which is lower than our $T_N$. Furthermore, we show the temperature dependence of the low-temperature specific heat of our as-grown single crystal in Fig. 6. We have clearly observed two successive peaks. This observation in the temperature dependence of the low-temperature specific heat is very comparable with that of $Yb_5Ir_4Si_{10}$ polycrystalline sample which is reported in Ref. [27]. But we have clearly observed *a shoulder* around 2K together with the sharp peak at $T_N = 3.5$ K in our SSE processed $Er_5Ir_4Si_{10}$ single crystal. In addition, we show the temperature-higher peak of the as-grown single crystal in Fig. 7. As it is clearly shown in Fig. 7, the temperature-higher peak has been observed at a little lower temperature than 3.5 K. These results verify that the SSE process is indispensible in order to improve the quality of the as-grown single crystals grown by Czochoralski pulling method.

On the other hand, Li et al. have reported on the superconductivity of $Sc_5Ir_4Si_{10}$ single crystal grown by the floating zone method [13]. Those single crystals have clearly showed anisotropic superconducting properties which are very well explained in the standard BCS model. Furthermore, we must note that the observation of the peak effect in the superconducting state is the direct evidence of the quasi-two-dimensional character of the crystal structure [30]. The observation of the peak effect in $Sc_5Ir_4Si_{10}$ single crystal grown by the floating method is very consistent with our study of the antiferromagnetic properties in our SSE processed $Er_5Ir_4Si_{10}$ single crystal grown by Czochoralski pulling method by using a tetra-arc furnace under high-purity argon atmosphere.

## 4. Conclusion

The AC magnetization measurement of the SSE processed $Er_5Ir_4Si_{10}$ single crystals combined with the experimental results of the low-temperature specific heat have revealed the experimental evidences for the following conclusions:

(1) $Er_5Ir_4Si_{10}$ single crystal is a quasi-two-dimensional material.
(2) $Er_5Ir_4Si_{10}$ single crystal is a quasi-two-dimensional antiferromagnet.
(3) $Er_5Ir_4Si_{10}$ single crystal exhibits an antiferromagnetic long-range ordering in the plane perpendicular to the *c*-axis of the tetragonal crystal structure, whereas there is no three-dimensional magnetic structure of $Er^{3+}$ local moments.
(4) The remarkable crystalline-electric-field effect is only observed in the plane which is perpendicular to the *c*-axis of the tetragonal crystal structure.
(5) In order to clarify the intrinsic magnetic properties, we need the high-resolution measurement of the low-temperature specific heat together with the magnetization measurement.
(6) The SSE process is indispensible in order to clarify the intrinsic magnetic properties of the single crystals grown by Czochoralski pulling method because the SSE process improves the quality of the as-grown single crystals.

Finally, we strongly insist that the structural phase transition of $Lu_5Ir_4Si_{10}$ single crystal is much the same as the cubic-tetragonal phase transition in A15 compounds because the nature of the phase transition in both compounds is the first-order one [9,23,31].

## References

[1] G.K. Shenoy, B.D. Dunlap, F.Y. Fradin (Eds.), Ternary Superconductors, Elsevier, North Holland, Amsterdam, The Netherland, 1981, pp. 239–242.
[2] S. Ramakrishnan, K. Gosh, G. Chandra, Phys. Rev. B 45 (1992) 10769.
[3] S. Ramakrishnan, K. Gosh, G. Chandra, Phys. Rev. B 46 (1992) 2958.
[4] K. Gosh, S. Ramakrishnan, G. Chandra, Phys. Rev. B 48 (1993) 4152.
[5] S. Ramakrishnan, K. Gosh, A.D. Chinchure, K. Jonason, V.R. Marathe, G. Chandra, Phys. Rev. B 51 (1995) 8398.
[6] K. Katoh, T. Tsutsumi, K. Yamada, G. Terui, Y. Niide, A. Ochiai, Physica B 373 (2006) 111.
[7] K. Tsutsumi, S. Takayanagi, K. Maezawa, H. Kitazawa, J. Alloys Comp. 453 (2008) 55.
[8] L.S. Hausermann-Berg, R.N. Shelton, Phys. Rev. B 35 (1987) 4673.
[9] L.S. Hausermann-Berg, R.N. Shelton, Phys. Rev. B 35 (1987) 6659.
[10] H.D. Yang, R.N. Shelton, H.F. Braun, Phys. Rev. B 33 (1986) 5062.

[11] R.N. Shelton, L.S. Hausermann-Berg, P. Klavins, H.D. Yang, M.S. Anderson, C.A. Swenson, Phys. Rev. B 34 (1986) 4590.
[12] T. Koyama, H. Sugita, S. Wada, K. Tsutsumi, J. Phys. Soc. Jpn. 68 (1999) 2326.
[13] G.J. Li, M. Miura, Z.X. Shi, T. Tamegai, Physica C 463–465 (2007) 76.
[14] H.F. Braun, C.U. Segre, Solid State Commun. 35 (1980) 735.
[15] H.F. Braun, K. Yvon, R.M. Braun, Acta Crystallogr. B 36 (1980) 2397.
[16] F. Galli, T. Taniguchi, A.A. Menovsky, G.J. Nieuwenhuys, J.A. Mydosh, S. Ramakrishnan, Physica B 281 & 282 (2000) 171.
[17] F. Galli, S. Ramakrishnan, T. Taniguchi, G.J. Nieuwenhuys, J.A. Mydosh, S. Geupel, J. Ludecke, S. van Smaalen, Phys. Rev. Lett. 85 (2000) 158.
[18] F. Galli, R. Feyerherm, R.W.A. Hendrix, S. Ramakrishnan, G.J. Nieuwenhuys, J.A. Mydosh, Phys. Rev. B 62 (2000) 13840.
[19] Y. Singh, S. Ramakrishnan, Physica B 359–361 (2005) 494.
[20] M.H. Jung, H.C. Kim, A. Migliori, F. Galli, J.A. Mydosh, Phys. Rev. B 68 (2003) 132102.
[21] H.D. Yang, P. Klavins, R.N. Shelton, Phys. Rev. B 43 (1991) 7688.
[22] S. van Smaalen, M. Shaz, L. Palatinus, P. Daniels, F. Galli, G.J. Nieuwenhuys, J.A. Mydosh, Phys. Rev. B 69 (2004) 014103.
[23] B. Becker, N.G. Patil, S. Ramakrishnan, A.A. Menovsky, G.J. Nieuwenhuys, J.A. Mydosh, M. Kohgi, K. Iwasa, Phys. Rev. B 59 (1999) 7266.
[24] J.B. Betts, A. Migliori, G.S. Boebinger, H. Ledbetter, F. Galli, J.A. Mydosh, Phys. Rev. B 66 (2002) 060106.
[25] Y.K. Kuo, Y.Y. Chen, L.M. Wang, H.D. Yang, Phys. Rev. B 69 (2004) 235114.
[26] Y.-K. Kuo, F.H. Hsu, H.H. Li, H.l. Haung, C.W. Haung, C.S. Lue, H.D. Yang, Phys. Rev. B 67 (2003) 195101.
[27] Z. Hossain, M. Schmidt, W. Schnelle, H.S. Jeevan, C. Geibel, S. Ramakrishnan, J.A. Mydosh, Y. Grin, Phys. Rev. B 71 (2005) 060406.
[28] S. Ramakrishnan, J.A. Mydosh, J. Magn. Magn. Mater. 310 (2007) 207.
[29] F. Galli, G.J. Nieuwenhuys, D.E. MacLaughlin, R.H. Heffner, A. Amato, O.O. Bernal, J.A. Mydosh, Physica B 319 (2002) 282.
[30] H.A. Radovan, N.A. Fortune, T.P. Murphy, S.T. Hannahs, E.C. Palm, S.W. Tozer, D. Hall, Nature 425 (2003) 51.
[31] B.T. Matthias, T.H. Geballe, Rev. Mod. Phys. 35 (1963) 1.